Supporting Information

High-speed AFM imaging reveals DNA capture and loop extrusion dynamics by cohesin-NIPBL

Parminder Kaur[1,2,*], Xiaotong Lu[3], Qi Xu[4,5], Elizabeth Marie Irvin[6], Colette Pappas[7], Hongshan Zhang[8], Ilya J. Finkelstein[8], Zhubing Shi[4,5], Yizhi Jane Tao[3], Hongtao Yu[4,5], Hong Wang[1,2,6,*]

[1]Physics Department, [2]Center for Human Health and the Environment, [6]Toxicology Program, [7]Biological Sciences, North Carolina State University, Raleigh, NC, USA

[3]Department of BioSciences, Rice University, Houston, TX, USA

[4] Westlake Laboratory of Life Sciences and Biomedicine, [5]School of Life Sciences, Westlake University, Hangzhou, Zhejiang Province, P.R. China

[8]Department of Molecular Biosciences, [9]Institute for Cellular and Molecular Biology, University of Texas at Austin, Austin, TX, USA

Video S1. HS-AFM video showing dynamics of the WT cohesin^{SA1}-NIPBL^{c} and extension of the arm-hinge domain to capture a DNA segment in proximity (4 mM ATP). Related to Figure 3B.

Video S2. HS-AFM video showing that a DNA-bound WT cohesin^{SA1}-NIPBL^{c} complex captures a DNA segment in proximity through the arm-hinge domain and initiates a DNA loop (4 mM ATP). Related to Figure 4 (II to VII).

Video S3. HS-AFM video showing dynamics of cohesin^{SA1}-NIPBL^{c} ATPase mutant and diffusion on DNA through short protrusions (4 mM ATP). Related to Figures 5A and S5.

Video S4. HS-AFM video demonstrating diffusion on DNA through short protrusions and arm extension by the cohesin^{SA1}-NIPBL^{c} ATPase mutant (4 mM ATP). Related to Figure 5B.

Video S5. HS-AFM video showing DNA capture by the cohesin^{SA1}-NIPBL^{c} ATPase mutant through arm extension (4 mM ATP). Related to Figure 5C.

Video S6. HS-AFM video showing DNA loop extrusion by WT cohesin^{SA1}-NIPBL^{c} (4 mM ATP). Related to Figure 7C.

Video S7. HS-AFM video showing DNA loop extrusion by WT cohesin^{SA1}-NIPBL^{c} (4 mM ATP). Related to Figure 7D.

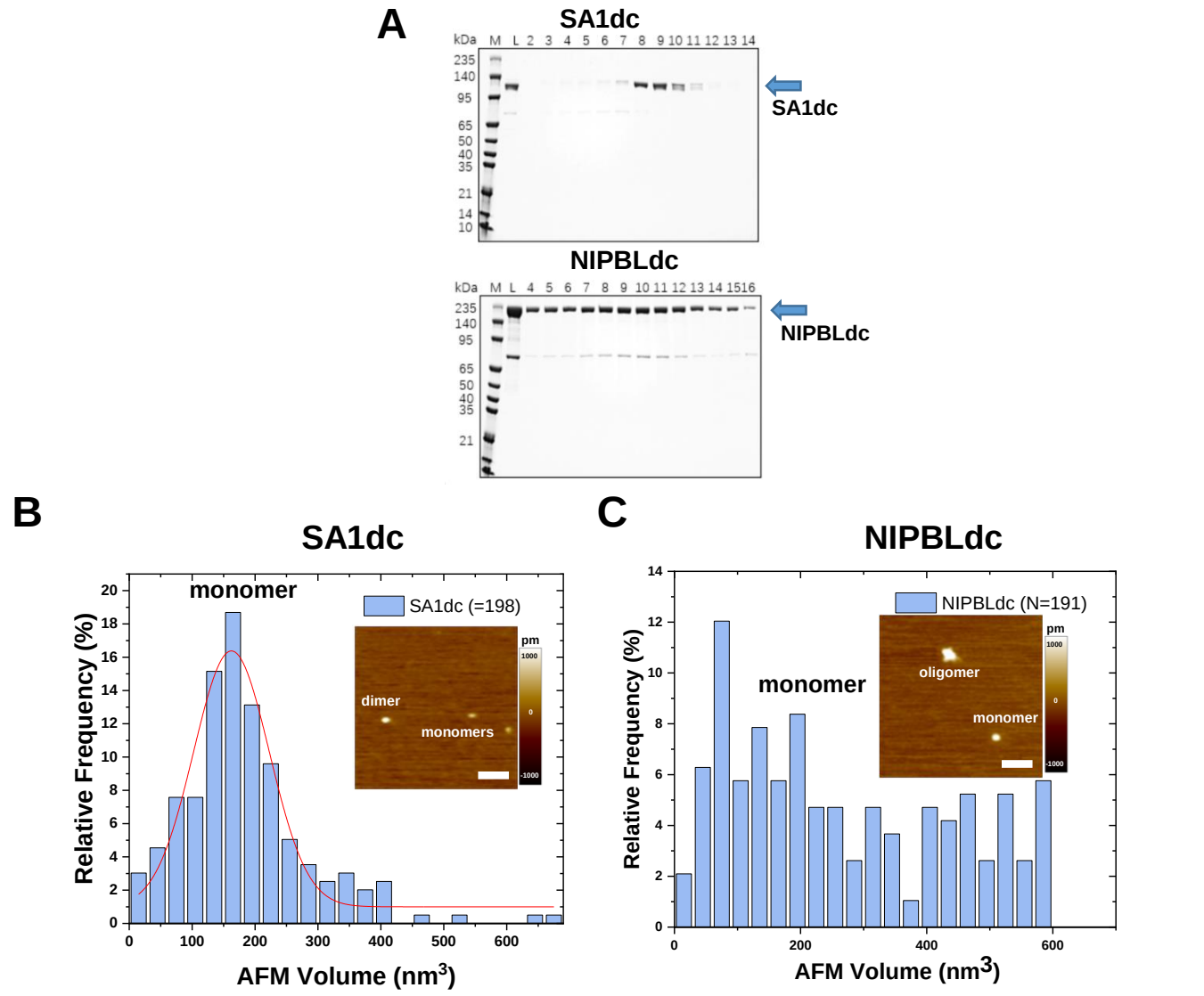

Figure S1. AFM volume analysis of SA1dc and NIPBLdc. *A,* SDS-PAGE of purified SA1dc and NIPBLdc. M: molecular marker. L: load. Numbers are fractions from the last FPLC purification step. *B* and *C*, Histograms of AFM volumes of SA1dc (B) and NIPBLdc (C, <600 nm^3). The red line represents Gaussian fit to the data with the peak centered at 162 nm^3 ± 120 nm^3 (R^2 > 0.90) for SA1dc. Based on the peak, the estimation of the molecular weight is 133 KDa for SA1dc, which is close to monomers. This estimation is based on a previously established calibration curve: V (nm^3) = 1.45 MW -21.57, where V is AFM volume and MW is molecular weight (Kaur et al. Scientific Reports, 2016). Inserts show example AFM images. The complexes with volumes greater than 300 nm^3 are treated as dimers and higher-order complexes. XY scale bar represents 100 nm.

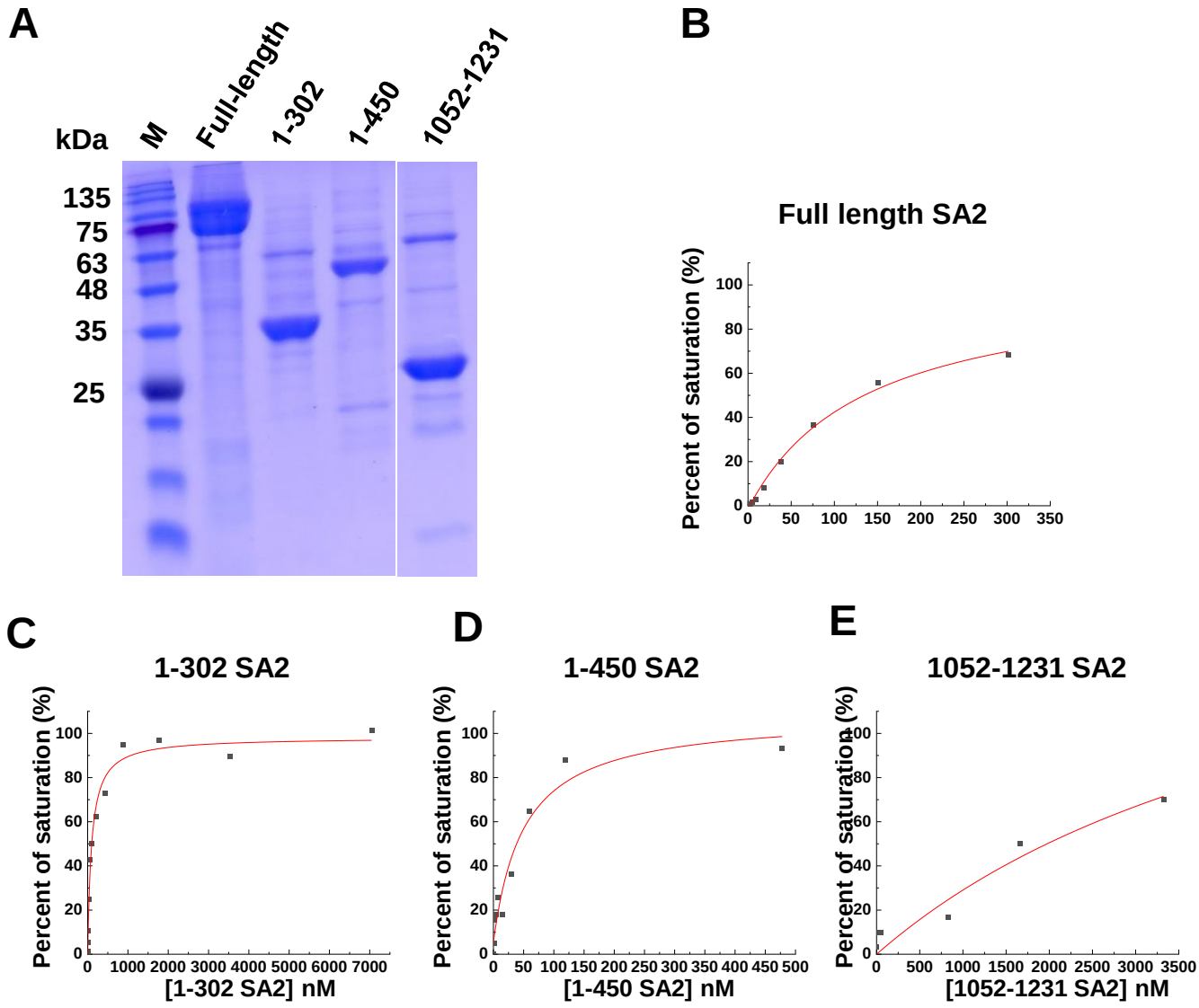

Figure S2. DNA binding by the full-length and truncation mutants of SA2. *A*, SDS-PAGE of the SA2 full length (1-1231 AAs), 1-302 AAs, 1-450 AAs, and 1052-1231 AAs. M: Molecular weight marker. The picture is cut from the same gel. *B* to *E*, Binding of the full length (*B*), 1-302 (*C*), 1-450 (*D*), and 1052-1231 (*E*) SA2 to 45 bp dsDNA measured by fluorescence anisotropy. dsDNA is labeled with Alexa 488. The data were fitted to the law of mass action (red lines, R^2 >0.9).

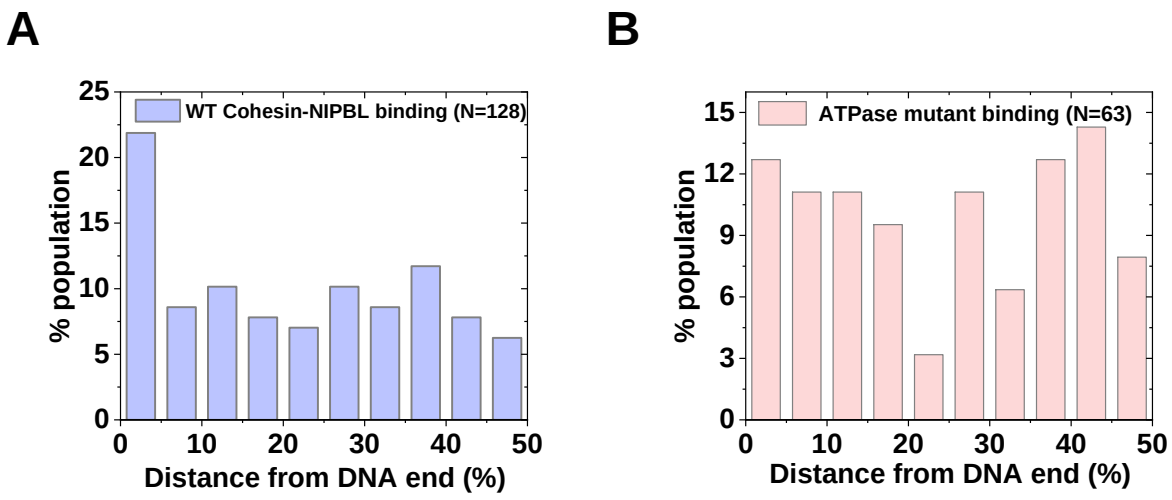

Figure S3. DNA binding position distributions of WT and ATPase mutant cohesin^{SA1}-NIPBL^{c} on linear dsDNA. *A* and *B*, Position distributions of WT (*A*) and ATPase mutant (*B*) cohesin^{SA1}-NIPBL^{c} on a linear dsDNA substrate (5.19 kb). Two independent experiments in the presence of 2.5 mM ATP.

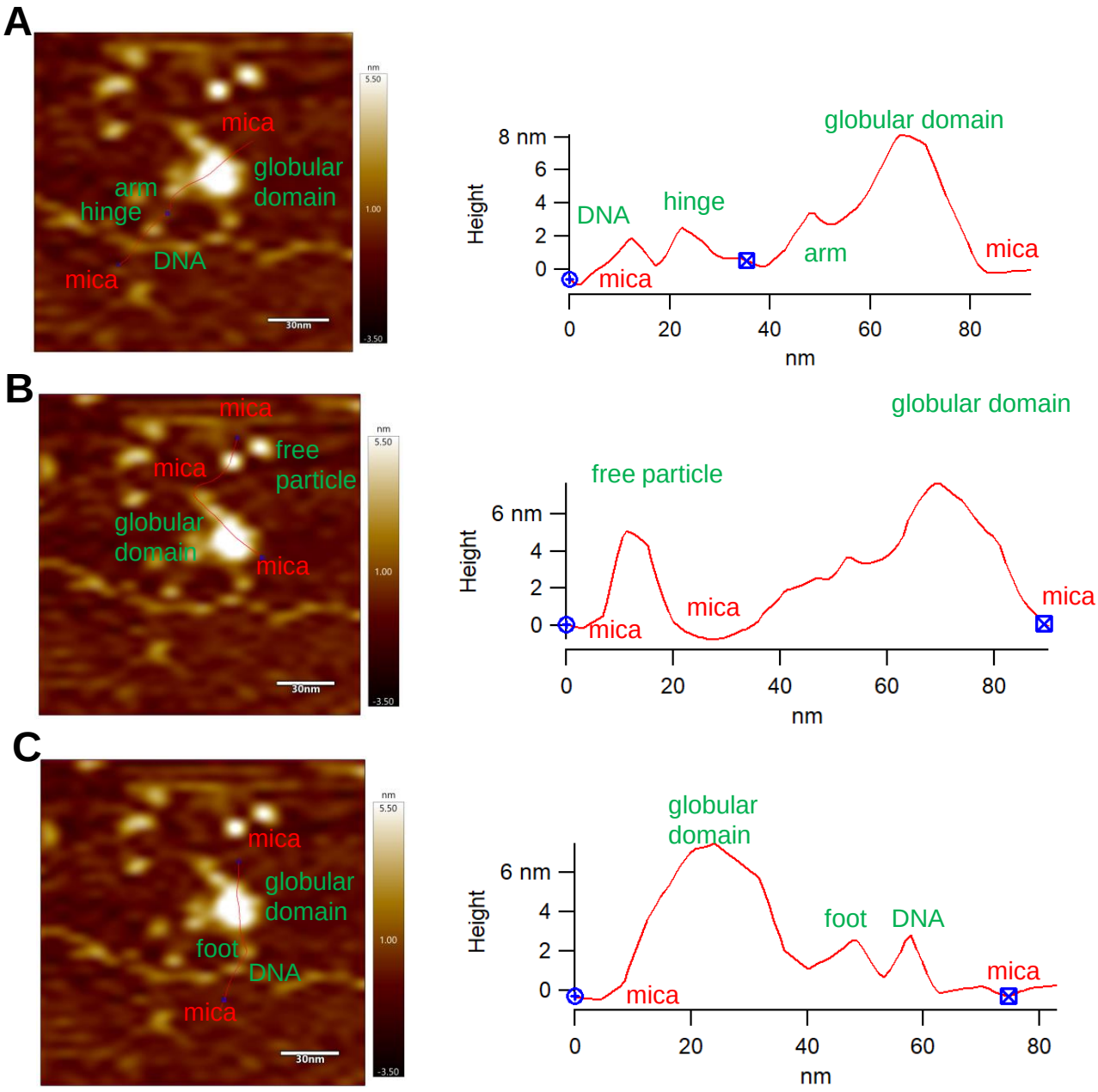

Figure S4. AFM height profile analysis showing hinge contacting DNA (*A*), a free particle (*B*), and foot connected to the globular domain contacting the DNA (*C*). Left panels: AFM images with the cross-sectional analysis lines in red and structural features labeled. Right panels: Cross-sectional analysis (height profile, red lines) with structural features labeled. Figures S4A-4C are re-use of the panel IV from Figure 3B for showing the height profiles at different regions.

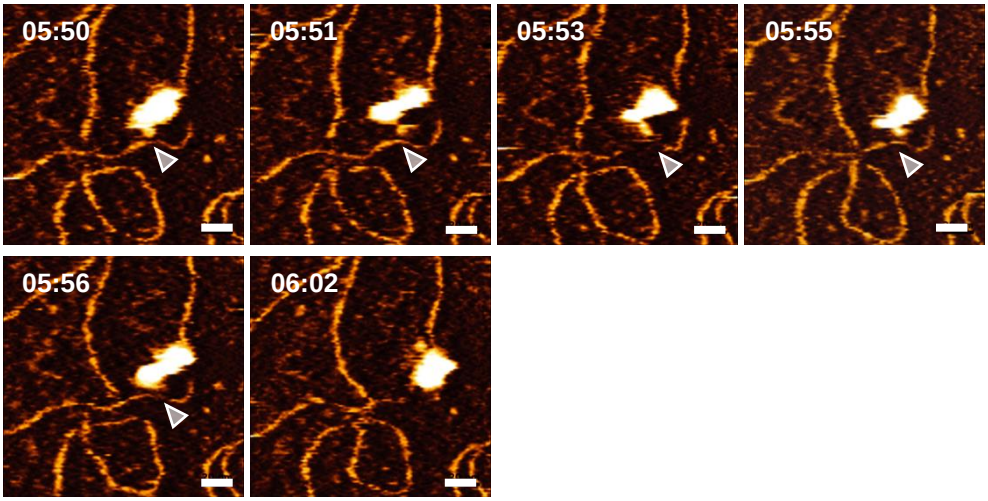

Figure S5. Time-lapse HS-AFM images of cohesin^{SA1}-NIPBL^{c} ATPase mutant walking (diffusion) on DNA through short protrusions. XY scale bar represents 20 nm. Also see **Video S3**. Observation times are in continuation of Figure 5A for the same molecules. *gray arrow: foot*. Time: min:s.

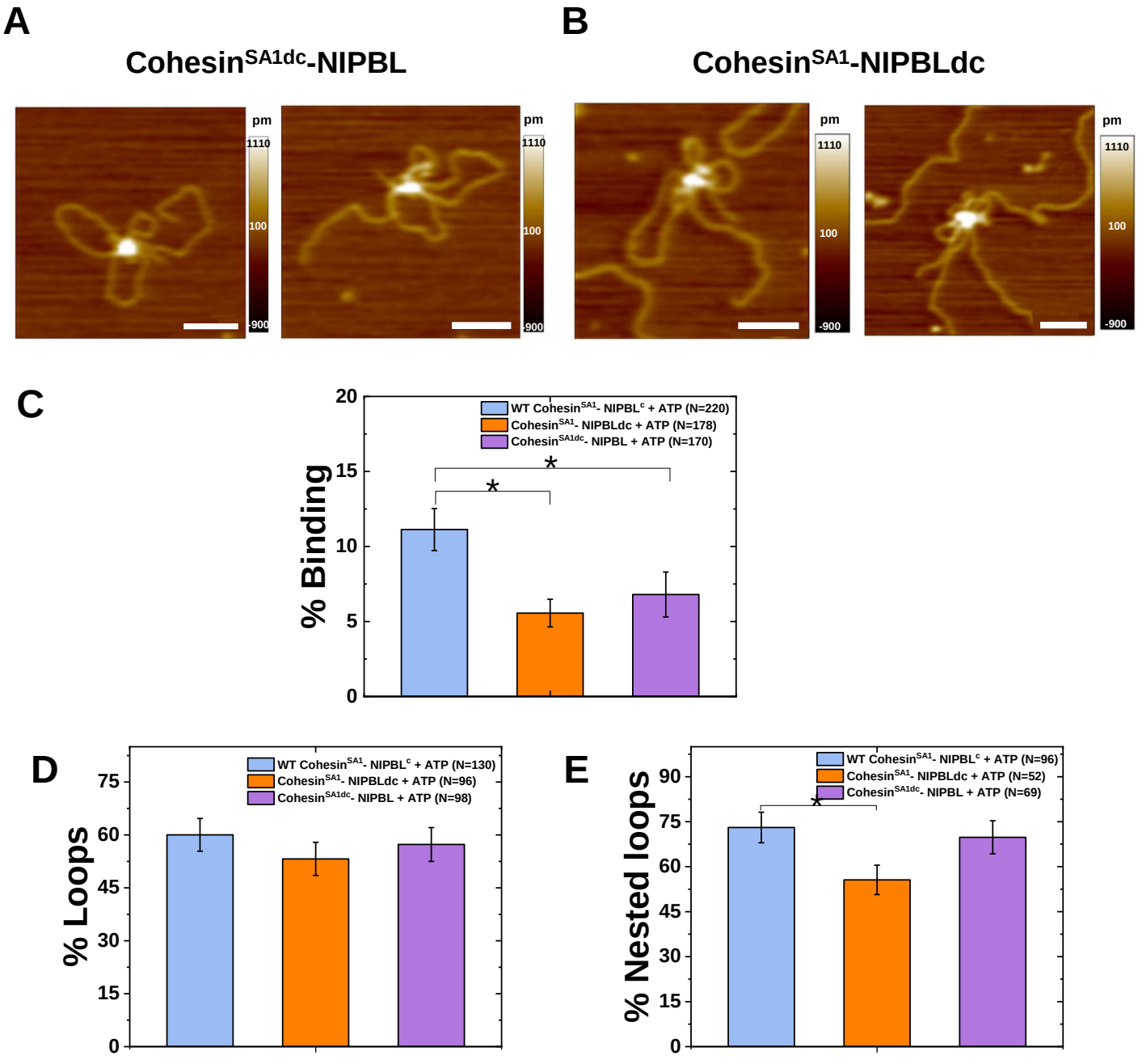

Figure S6: DNA binding and loop formation mediated by cohesin-NIPBL missing the C-terminal domain of either SA1 or NIPBL. *A* and *B*, Representative AFM images of DNA loops mediated by cohesin^{SA1dc}-NIPBL (*A*) and cohesin^{SA1}-NIPBLdc (*B*) in the absence of ATP. Cohesin^{SA1}-NIPBL: 30 nM. DNA (5.19 kb): 6 nM. XY scale bar represents 100 nm. *C* to *E*, Quantification of the percentages of DNA molecules bound with cohesin-NIPBL molecules (*C*), DNA loops (D), and nested loops out of total DNA loops mediated by WT, cohesin^{SA1dc}-NIPBL, and cohesin^{SA1}-NIPBLdc complexes. Error bars: SD. At least 3 experiments for each condition. * $p<0.05$ based on Student's t-test. The data for WT cohesin^{SA1}-NIPBL^{c} is from a different batch of protein compared to the data presented in Figure 6.

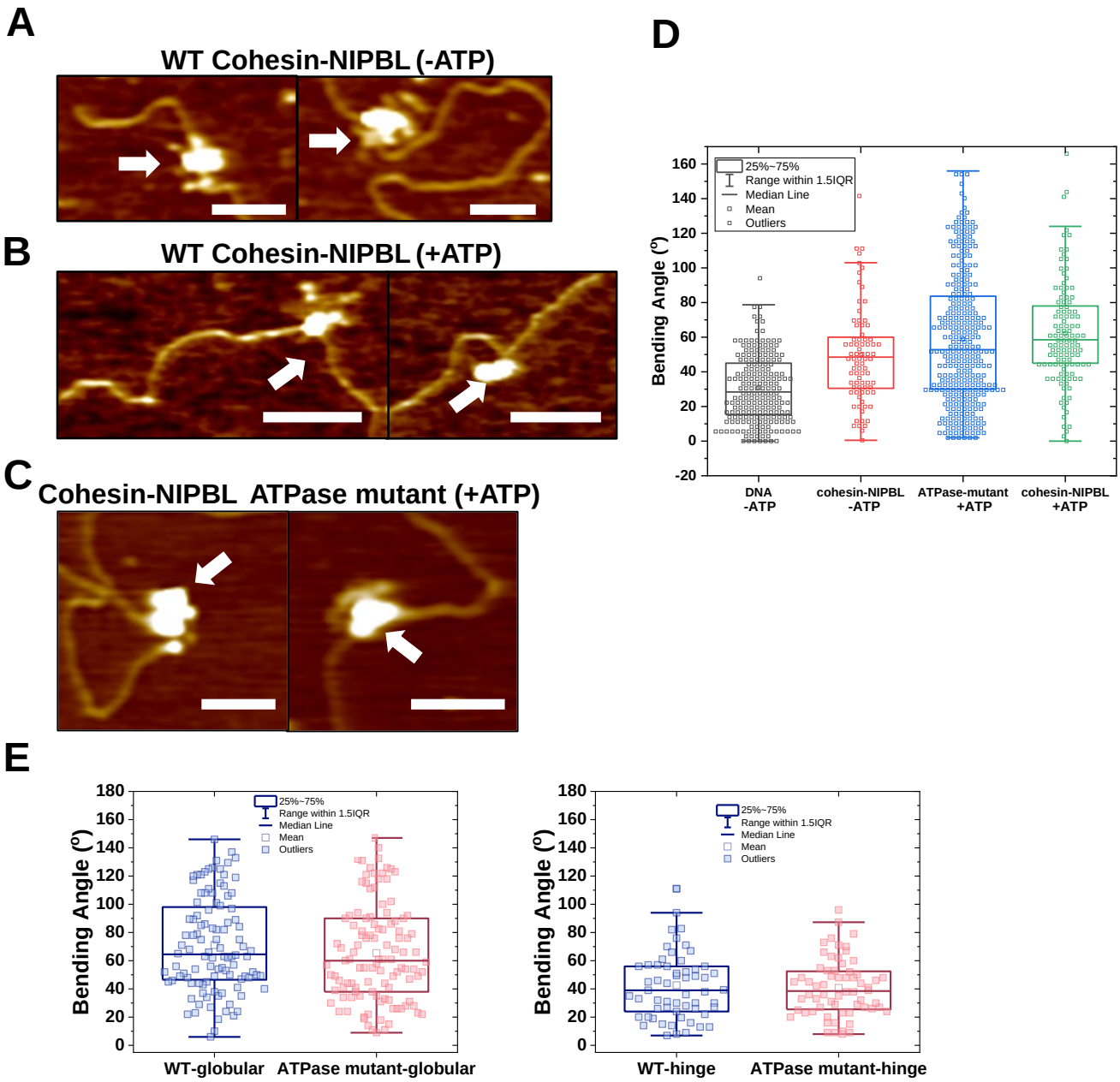

Figure S7. Cohesin^{SA1}-NIPBL^{c} binding induces DNA bending. *A* to *C*, Representative AFM images of WT cohesin^{SA1}-NIPBL^{c} in the absence (*A*), or presence of ATP (+2.5 mM, *B*), and cohesin^{SA1}-NIPBL^{c} ATPase mutant (+2.5 mM ATP, *C*) with dsDNA (5.19 kb). White arrows point to protein-DNA complexes. XY scale bar represents 100 nm. *D*, DNA bending angles induced by the WT and ATPase mutant of cohesin^{SA1}-NIPBL^{c} on dsDNA. DNA bending angles: 27.5° (± 26°) for DNA_{+ATP} (N=149), 43.7° (± 20.5°) for DNA_{WT-ATP} (N=80), 57.2° (± 27.6°) for DNA_{WT+ATP} (N=116), and 47.3° (± 41.0°) for $DNA_{ATPase\ mutant+ATP}$ (N=298). *E*, DNA bending angles induced by the globular domain (left panel) of the WT (71.2° ± 33.6°, N=104) and ATPase mutant (65.4° ± 34.6°, N=111), and the hinge domain (right panel) of WT (42.6° ± 24.4°, N=59) and ATPase mutant (40.7° ± 20.3°, N=104) cohesin^{SA1}-NIPBL^{c}.

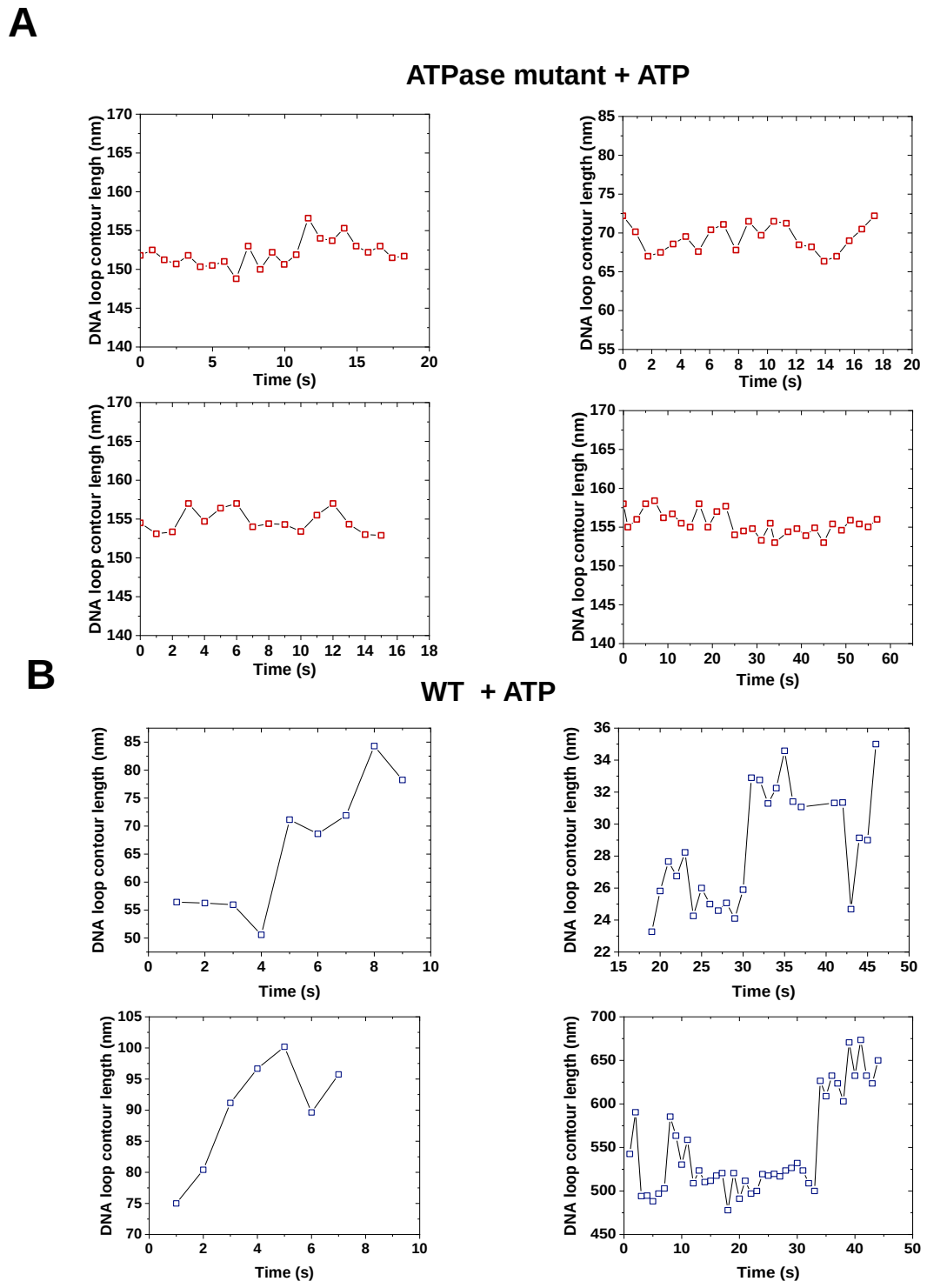

Figure S8. DNA loop length changes mediated by the ATPase mutant and WT cohesin^{SA1}-NIPBL^{c} on linear dsDNA in the presence of ATP . *A*, Frame-to-frame DNA loop lengths versus time for four independent DNA loops mediated by the cohesin^{SA1}-NIPBL^{c} ATPase mutant (4 mM ATP). *B*, Additional examples of frame-to-frame DNA loop lengths versus time mediated by WT cohesin^{SA1}-NIPBL^{c} (4 mM ATP).

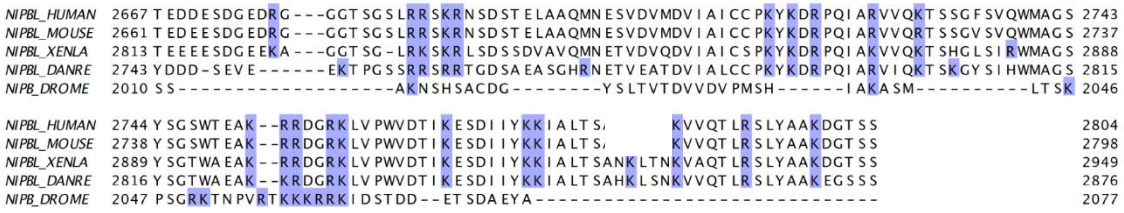

Figure S9. The C-terminal domain of NIPBL contains conserved positively charged residues. Alignment of sequences at the C-terminus of NIPBL from different species. Positively charged residues are highlighted in blue.